Microstructure of Mn-doped γ-Ga_2O_3 epitaxial film on sapphire (0001) with room temperature ferromagnetism

Rong Huang, Hiroyuki Hayashi, Fumiyasu Oba, and Isao Tanaka[a)]
Department of Materials Science and Engineering, Kyoto University, Yoshida, Sakyo, Kyoto 606-8501, Japan

(Received 16 November 2006; accepted 20 January 2007; published online 26 March 2007)

Mn-doped Ga_2O_3 thin film showing room temperature ferromagnetism has been grown on a sapphire (0001) plane by using a pulsed-laser deposition technique. The microstructure of the Mn-doped film is investigated in detail using selected-area electron diffraction, high-resolution transmission electron microscopy (HRTEM), x-ray energy-dispersive spectroscopy, and electron energy-loss spectroscopy, in comparison with an undoped film. Careful diffraction analysis with the $[2\bar{1}\bar{1}0]_{Al_2O_3}$ and $[10\bar{1}0]_{Al_2O_3}$ zone axes of the substrates reveals that the Mn-doped film shows the γ-Ga_2O_3 phase with a defective spinel structure, while the undoped film shows the β-Ga_2O_3 phase. The orientation relationship between the film and substrate is determined by electron diffraction and HRTEM from the interface region to be $(\bar{2}01)_{\beta\text{-}Ga_2O_3}//(0001)_{Al_2O_3}$ and $[102]_{\beta\text{-}Ga_2O_3}//[2\bar{1}\bar{1}0]_{Al_2O_3}$ or $[\bar{1}0\bar{2}]_{\beta\text{-}Ga_2O_3}//[2\bar{1}\bar{1}0]_{Al_2O_3}$ for the undoped film, and $(111)_{\gamma\text{-}Ga_2O_3}//(0001)_{Al_2O_3}$ and $[2\bar{1}\bar{1}]_{\gamma\text{-}Ga_2O_3}//[2\bar{1}\bar{1}0]_{Al_2O_3}$ or $[\bar{2}11]_{\gamma\text{-}Ga_2O_3}//[2\bar{1}\bar{1}0]_{Al_2O_3}$ for the Mn-doped film. Mn ions are uniformly dissolved in the film with 7.8 cation % and no detectable precipitates are found. Mn-$L_{2,3}$ energy-loss near-edge structure reveals that Mn ions take the valency of 2+, which is consistent with Mn-$L_{2,3}$ near edge x-ray absorption results in our previous report. © *2007 American Institute of Physics*. [DOI: 10.1063/1.2713349]

I. INTRODUCTION

With potential applications in spintronic devices, such as fast nonvolatile semiconductor memories and integrated magnetic/electronic/photonic devices, diluted magnetic semiconductors (DMS) that involve charge and spin degrees of freedom in a single material have attracted increasing research interests since the ferromagnetism in $In_{1-x}Mn_xAs$ (Ref. 1) and $Ga_{1-x}Mn_xAs$ (Ref. 2) was discovered. However, low magnetic ordering temperature in these systems restricts its spintronic applications at room temperature.[3,4] Following Dietl's theoretical prediction that transition-metals (especially Mn) doped wide-band gap semiconductors (GaN and ZnO) with high hole concentration could achieve high T_c exceeding room temperature,[5] numerous works have been carried out recently.[6–11] In 2002, Mn-doped GaN films with room-temperature ferromagnetism have been made.[12] The estimated Curie temperature is as high as 940 K at 5.7% of Mn. Even though tremendous progress has been made on GaN, it is worth exploiting other categories of DMS with room-temperature ferromagnetism because the mechanism of the ferromagnetism is still controversial.

Gallium oxide is a wide-band gap oxide semiconductor with potential technical applications for optoelectronic devices. Several polymorphs are well known for gallium oxide as α, β, γ, δ, and ε.[13] They are different not only in their crystal space group but also in the coordination number (CN) of Ga ions. β-Ga_2O_3 is most commonly available monoclinic crystal with lattice parameters of $a=1.223$, $b=0.304$, $c=0.580$ nm, $\beta=103.7°$, and the $C2/m$ space group,[14] which shows the same number of CN=4 and CN=6 sites. γ-Ga_2O_3 is analogous to γ-Al_2O_3 and has defective cubic spinel structure ($MgAl_2O_4$-type) with a lattice parameter of $a=0.822$ nm and the $Fd\bar{3}m$ space group.[15] It also has both CN=4 and CN=6 sites. Recently, β-Ga_2O_3 thin films have been obtained by different methods.[16–19] Mn-doped Ga_2O_3 has been studied for application as luminescent materials. It is known to exhibit green-color photoluminescence (PL) at 490 nm. The presence of Mn^{2+} is thought to be essential for the PL, which is abundant only after annealing the sample in Ar atmosphere at temperatures between 1000 and 1300 °C.[20]

Recently, we reported epitaxial growth of ferromagnetic Mn-doped Ga_2O_3 thin film by the pulsed-laser deposition (PLD) technique.[21] The film was found to have Curie temperature higher than 350 K. In the present study, the Mn-doped film is investigated in detail by using selected-area electron diffraction (SAD), high-resolution transmission electron microscopy (HRTEM), x-ray energy-dispersive spectroscopy (EDS), and electron energy-loss spectroscopy (EELS). Microstructure, crystalline phase, and orientation relationship are discussed in comparison with an undoped film. The concentration and valence of Mn is determined by the spectroscopic techniques.

II. EXPERIMENTAL PROCEDURES

Thin film samples were prepared by a PLD method using an excimer KrF* laser source ($\lambda=248$ nm, $\tau=25$ ns, Lambda physik COMPex205) with a power of 3×10^4 J m^{-2} and a repetition frequency of 10 Hz. Al_2O_3(0001) single crystal was used for the substrate, which was kept at 773 K and $p_{O_2}=0.05$ Pa during the deposition. The oxygen pressure was increased after the deposition to

a)Electronic mail: tanaka@cms.MTL.kyoto-u.ac.jp

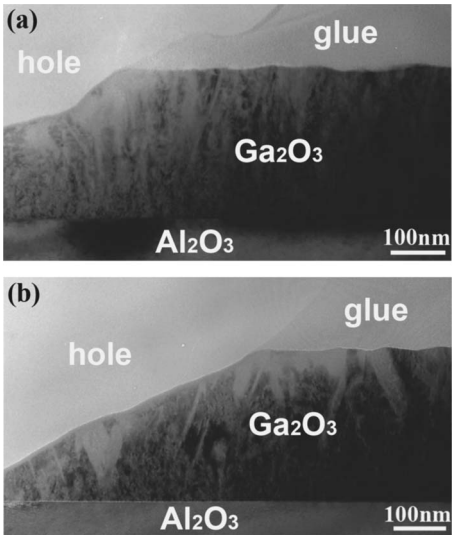

FIG. 1. Cross-section TEM bright-field images. (a) Undoped Ga_2O_3 film. (b) Mn-doped Ga_2O_3 film.

130 Pa and kept during cooling to the room temperature. β-Ga_2O_3 sintered with/without Mn was used as PLD targets, which were fabricated by the mixing of a commercially available high-purity powder of MnO_2 with Ga_2O_3 powder followed by sintering in air at 1623 K for 3 h.

Cross-section TEM specimens were prepared by a standard procedure which includes mechanical grinding, polishing, precision dimpling, and ion milling. The final thinning of specimens was carried out on an ion polishing system (PIPS, model 691, Gatan, Inc., Pleasanton, CA) using an accelerating voltage of 4.0 kV and an incident angle of 4°–6°. TEM observations were performed on an electron microscope with a field emission gun operated at 200 kV (CM200FEG, FEI, Eindhoven, the Netherlands), equipped with an imaging filter (GIF, Gatan, Inc., Pleasanton, CA) for EELS and an x-ray spectrometer (DX4, EDAX Inc., Mahwah, NJ) for EDS. Diffraction analyses were carried out partially on a conventional TEM (CM200, FEI, Eindhoven, the Netherlands). The diffraction patterns were simulated by using MacTempas software (Total Resolution, Berkeley, CA).

III. RESULTS AND DISCUSSION

A. Microstructure

Undoped and Mn-doped Ga_2O_3 thin films were obtained by the PLD method. $\theta-2\theta$ x-ray diffraction (XRD) analysis showed a single peak between 20° and 40°, located at 38.40° for the undoped film, which corresponds well to $\beta(\bar{4}02)$.[21] The Mn-doped film also showed a single peak at 37.60°, which can be ascribed to $\gamma(222)$ at 37.28° or $\beta(\bar{4}02)$.[21] No other peaks were detected. In order to identify the crystalline phase and microstructure, cross-section TEM investigations were carried out for both samples. Figure 1 shows resultant bright-field images. Both films have uniform and similar thickness of about 300 nm. The undoped film consists of fine columnar grains as recognized in Fig. 1(a). In contrast, the Mn-doped film shows larger grains with linear features that have about 70° angle with the interface. They are found to be twin boundaries as discussed later.

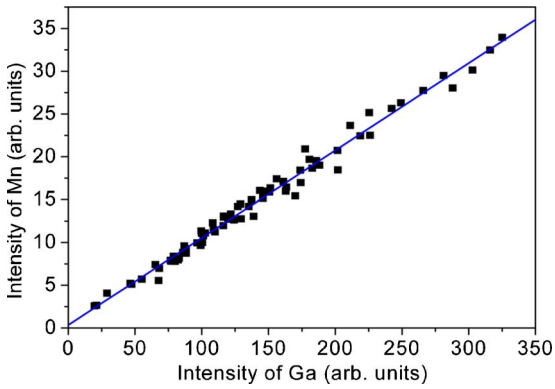

FIG. 2. Relationship of Mn intensity and Ga intensity measured by EDS from 73 points in the Mn-doped Ga_2O_3 thin film.

To measure the concentration of Mn in Mn-doped film, EDS analysis with probe size of about 1 nm in diameter has been performed on TEM. We scanned the film manually in both directions parallel and perpendicular to the interface in different sample areas with different thickness. Data at 73 points were obtained and plotted in Fig. 2. The horizontal and vertical axes are the peak intensity of Ga and Mn quantified by the commercial software on the DX4 system, respectively. The data show a good linear relation between Ga and Mn intensity with an *R*-squared value of 0.986, which means that Mn ions are uniformly dissolved in the thin film.[22] No detectable clusters of Mn or other Mn-rich precipitates are found. According to the Cliff–Lorimer equation,[23] the concentration of Mn in Ga_2O_3 film is quantified as 7.8±0.3 cation %, which is consistent with the result by scanning electron microscopy-EDS.[21]

B. Crystalline phase and orientation relationship in undoped film

The $\theta-2\theta$ XRD analysis can detect only peaks corresponding to a single plane group in epitaxial thin films. Therefore, there exist some uncertainties to identify the phase and orientation relationship. In the present work, SAD patterns from more than two zone axes are used to identify the phase in the film complementarily to the XRD analysis. Figure 3(a) shows a diffraction pattern when electron beam is parallel to the $[2\bar{1}\bar{1}0]$ direction of Al_2O_3. It can be indexed as $\beta[102]$ or $\gamma[2\bar{1}\bar{1}]$ zone axes, which are found to have a close resemblance despite the difference in crystal structure. The two phases are difficult to differentiate solely from these patterns. However, when we tilt the sample by 30° to the $[10\bar{1}0]$ zone axis of Al_2O_3, the diffraction pattern of the film as shown in Fig. 3(b) can be identified as superposition of three sets of patterns, I: [132], II: $[1\bar{3}2]$, and III: $[0\bar{1}0]$ of β-Ga_2O_3, arising from at least three grains orientated in respective directions in the selected area. Thus, β phase in the undoped thin film has been confirmed by the diffraction analyses.

Figure 4(a) shows SAD patterns from both of the film (solid line) and substrate (dashed line). The patterns clearly indicate the orientation relationship of $(\bar{2}01)_{\beta\text{-}Ga_2O_3}//(0001)_{Al_2O_3}$, and $[102]_{\beta\text{-}Ga_2O_3}//[2\bar{1}\bar{1}0]_{Al_2O_3}$ or $[\bar{1}02]_{\beta\text{-}Ga_2O_3}//[2\bar{1}\bar{1}0]_{Al_2O_3}$. Figure 4(b) is a HRTEM image of

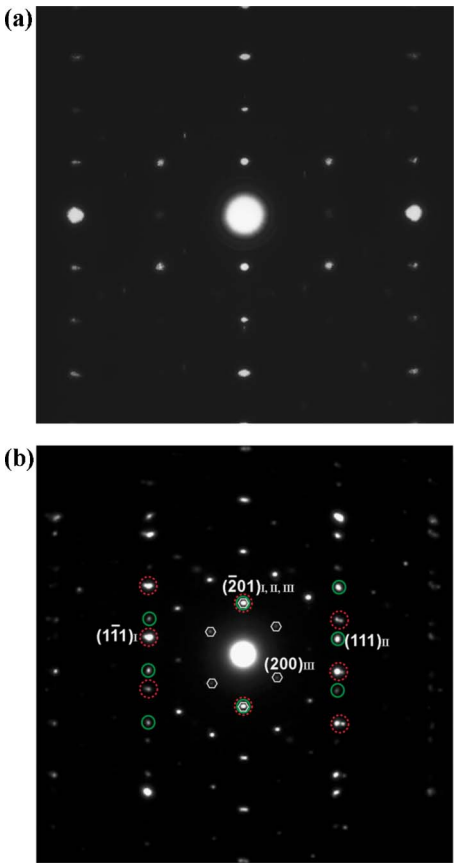

FIG. 3. Selected-area electron-diffraction patterns of undoped β-Ga_2O_3 film obtained from orientations parallel to (a) $[2\bar{1}\bar{1}0]_{Al_2O_3}$, and (b) $[10\bar{1}0]_{Al_2O_3}$. The patterns in (b) exhibit the superposition of three patterns with zone axes I: $[132]_{\beta\text{-}Ga_2O_3}$, II: $[1\bar{3}2]_{\beta\text{-}Ga_2O_3}$, and III: $[0\bar{1}0]_{\beta\text{-}Ga_2O_3}$, which are denoted by the dashed circle, solid circle, and hexagon, respectively.

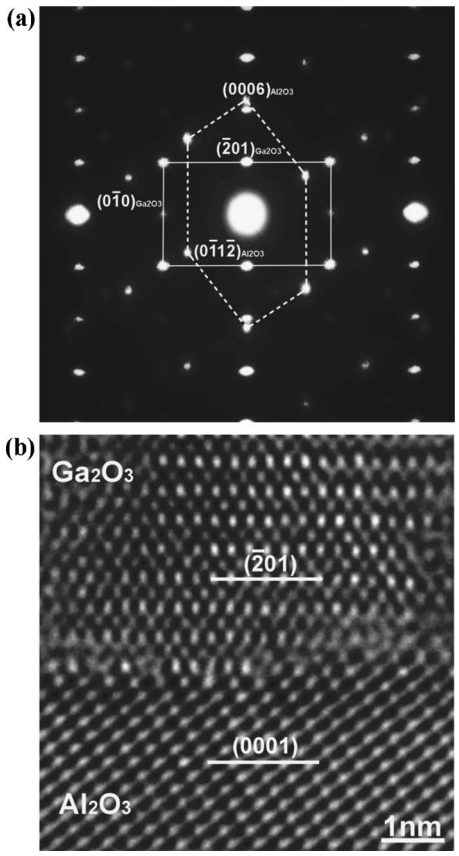

FIG. 4. (a) Selected-area electron diffraction patterns from both of undoped β-Ga_2O_3 film and Al_2O_3 substrate. The solid and dashed lines denote patterns from β-Ga_2O_3 film and Al_2O_3 substrate, respectively. (b) HRTEM image of the interface between β-Ga_2O_3 film and Al_2O_3 substrate.

the interface between the β-Ga_2O_3 film and the Al_2O_3 substrate, which confirms the epitaxial growth of the film in the earlier orientation relationship. While no previous reports on the in-plane orientation relationship can be found for this system, the out-of-plane relationship is consistent with previously reported XRD results.[17,21] In the monoclinic β-Ga_2O_3 crystal, the [102] and [010] directions are perpendicular to each other. The [102] and [132] directions and the [102] and $[1\bar{3}2]$ directions make an angle of 31.8°, which is close to the angle between $[2\bar{1}\bar{1}0]_{Al_2O_3}$ and $[10\bar{1}0]_{Al_2O_3}$, 30°. Because of the threefold symmetry of the (0001) plane of Al_2O_3, the earlier relationship involves three kinds of equivalent in-plane orientations of β-Ga_2O_3 grains. Figure 5(a) schematically shows the orientation configuration of β-Ga_2O_3 grains on (0001) plane of Al_2O_3 substrate. According to these orientation configurations, we simulated the diffraction pattern with electron beam parallel to $[10\bar{1}0]_{Al_2O_3}$ as shown in Fig. 5(b). This corresponds very well to the experimental diffraction pattern in Fig. 3(b).

C. Crystalline phase and orientation relationship in Mn-doped film

Similarly, we identified the crystalline phase in Mn-doped thin film. Figure 6(a) is a diffraction pattern from the film when electron beam is parallel to the $[2\bar{1}\bar{1}0]$ direction of Al_2O_3 substrate. This looks very similar to that from the undoped film [see Fig. 3(a)], apart from the difference in the intensity of diffraction spots. However, as shown in Fig. 6(b), the diffraction pattern obtained from the Mn-doped film is totally different from the pattern from the undoped film when we tilt the sample by 30° to the $[10\bar{1}0]_{Al_2O_3}$ zone axis. It can be indexed only as a superposition of I: $[\bar{1}0\bar{1}]$ and II: $[\bar{1}01]$ of γ-Ga_2O_3 among the polymorphs.[13] This is supported by extensive microdiffraction analyses made for many grains. An example of the results is given in the inset of Fig. 6(b). In addition, {111} twining in γ-Ga_2O_3 grains has been observed, which usually occurs during the grain growth of cubic structure. The presence of twin boundaries is confirmed by HRTEM, as shown in Fig. 7. In the bright-field image shown in Fig. 1(b), some {111} twins can be recognized as linear features making angles of about 70° with the γ-$Ga_2O_3(111)/Al_2O_3(0001)$ interface, corresponding to the angle of 70.5° between {111} planes. They are inclined toward left or right, which also indicates the coexistence of grains in the two orientations. This work unambiguously assigns the phase of the Mn-doped thin film to the γ-Ga_2O_3. The {111} twin boundary is considered coherent, hence, with low boundary energy. The segregation of Mn at the twin boundary should not be remarkable. The present nanoprobe EDS analysis actually found no detectable segregation.

The electron and x-ray diffraction analyses draw a consistent conclusion that Mn-doped γ-Ga_2O_3 is epitaxially

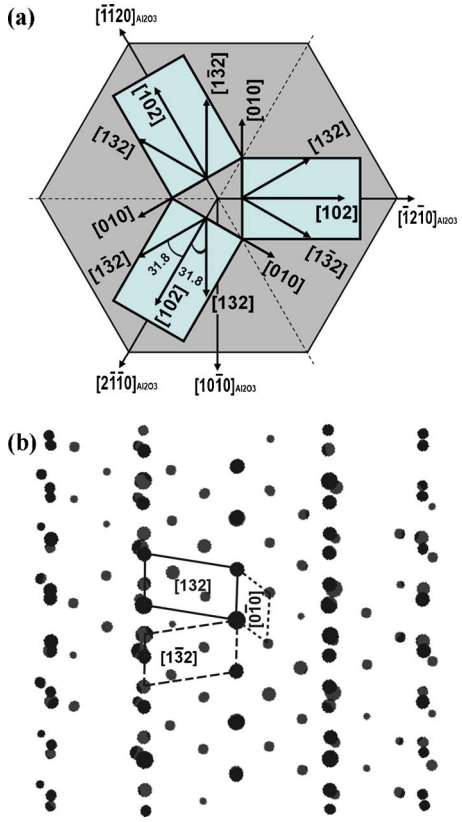

FIG. 5. (a) Schematic of the orientation configuration of β-Ga_2O_3 grains on $(0001)_{Al_2O_3}$ plane. (b) Simulated diffraction pattern with electron beam parallel to $[10\bar{1}0]_{Al_2O_3}$ according to the three orientation configurations shown in (a).

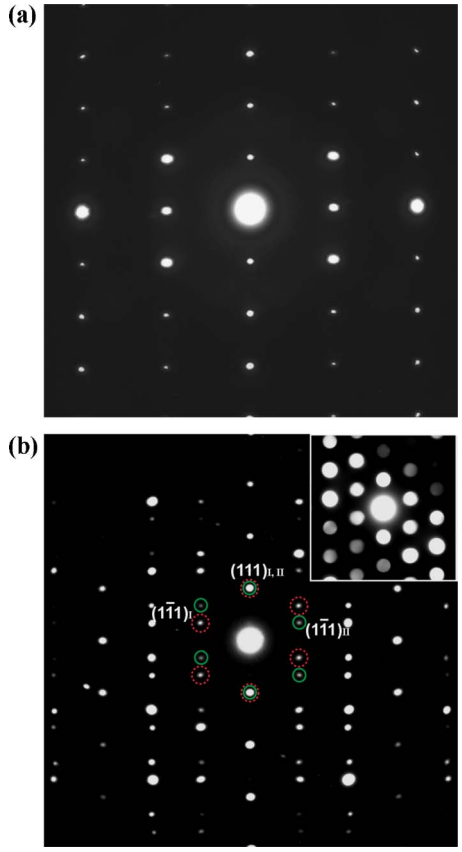

FIG. 6. Selected-area electron-diffraction patterns of Mn-doped γ-Ga_2O_3 film obtained from orientations parallel to (a) $[2\bar{1}\bar{1}0]_{Al_2O_3}$, and (b) $[10\bar{1}0]_{Al_2O_3}$. The patterns in (b) show twin crystal relationship between zone axes I: $[\bar{1}01]_{\gamma\text{-}Ga_2O_3}$ and II: $[\bar{1}01]_{\gamma\text{-}Ga_2O_3}$. The inset is a microdiffraction pattern from one grain.

grown on the $(0001)_{Al_2O_3}$ with an orientation relationship of $(111)_{\gamma\text{-}Ga_2O_3}//(0001)_{Al_2O_3}$, and $[2\bar{1}\bar{1}]_{\gamma\text{-}Ga_2O_3}//[2\bar{1}\bar{1}0]_{Al_2O_3}$ or $[\bar{2}11]_{\gamma\text{-}Ga_2O_3}//[2\bar{1}\bar{1}0]_{Al_2O_3}$, as confirmed by SAD patterns from both of the film (solid line) and Al_2O_3 substrate (dashed line) in Fig. 8(a). The high-resolution image displayed in Fig. 8(b) shows a direct contact of the γ-Ga_2O_3 and Al_2O_3 crystals at the interface without any precipitates. Because of the high symmetry of the (111) plane of the cubic structure, the earlier relationship involves only two kinds of equivalent in-plane orientations of γ-Ga_2O_3 grains. Figure 9(a) schematically shows the orientation configuration of γ-Ga_2O_3 grains on the (0001) plane of Al_2O_3 substrate. According to these two orientation configurations, the diffraction pattern with electron beam parallel to $[10\bar{1}0]_{Al_2O_3}$ has been simulated. The resultant pattern shown in Fig. 9(b) agrees very well with the experimental diffraction pattern [see Fig. 6(b)].

Ga_2O_3 has a polymorphism similar to that of Al_2O_3. Among the polymorphs of α, β, γ, δ and ε, β-Ga_2O_3 can be synthesized most easily. The other phases are obtained only under special conditions.[13] In the present work, the undoped β-Ga_2O_3 film is epitaxially grown on (0001) surface of Al_2O_3 by PLD method with pure β-Ga_2O_3 target, which is consistent with previous works reported in literature.[17] When 5 cation % of Mn is introduced into the target, the γ-Ga_2O_3 thin film with defective spinel structure and 7.8±0.3 cation % Mn is obtained under the same growth conditions. Synthesis of Ga_2O_3 with another crystal structure was recently reported in Sn-doped PLD thin film.[18] These results imply that the structure of Ga_2O_3 is very sensitive to doping and can be designed by introducing different additive elements, giving a new scenario for the application of Ga_2O_3 polymorphs.

D. Valency and coordination number of Mn

The 7.8 cation % Mn-doped thin film clearly exhibited ferromagnetism with a Curie temperature higher than 350

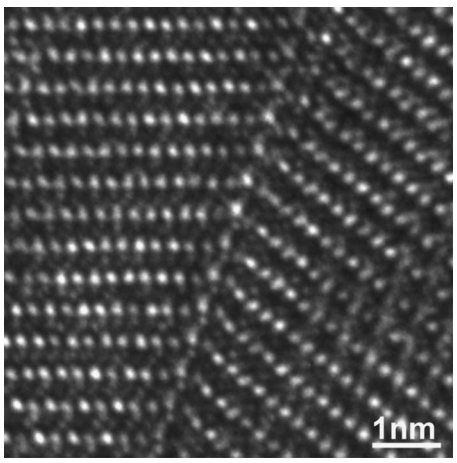

FIG. 7. HRTEM image showing a {111} twin boundary in Mn-doped γ-Ga_2O_3 film.

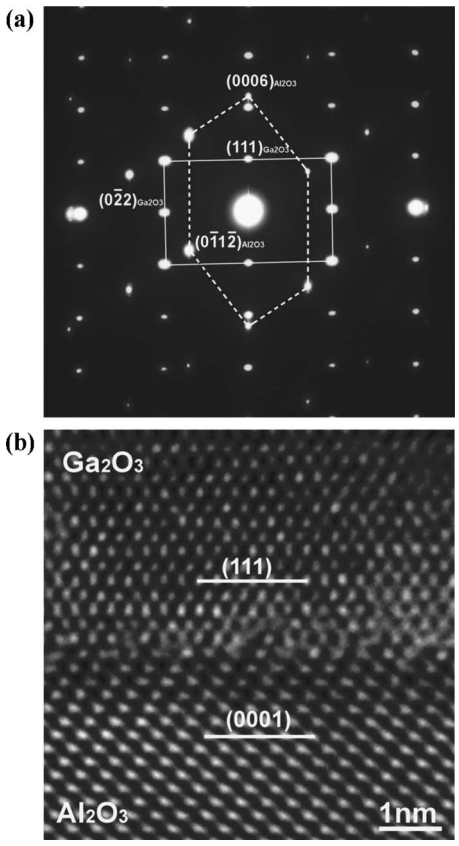

FIG. 8. (a) Selected-area electron diffraction patterns from both of γ-Ga_2O_3 film and Al_2O_3 substrate. The solid and dashed lines denote patterns from γ-Ga_2O_3 film and Al_2O_3 substrate, respectively. (b) HRTEM image of the interface between γ-Ga_2O_3 film and Al_2O_3 substrate.

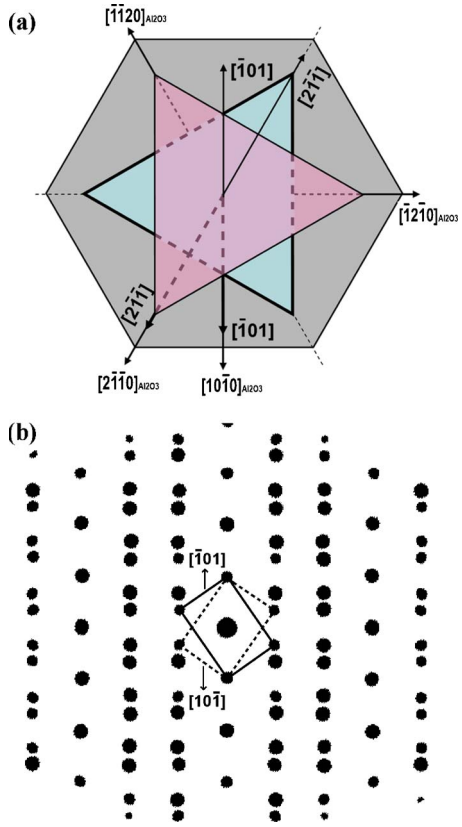

FIG. 9. (a) Schematic of the orientation configuration of γ-Ga_2O_3 grains on $(0001)_{Al_2O_3}$ plane. (b) Simulated diffraction pattern with electron beam parallel to $[10\bar{1}0]_{Al_2O_3}$ according to the two orientation configurations shown in (a).

K.[21] The valency of Mn is expected to play an important role on the magnetic properties, as reported for ferromagnetic $Ga_{1-x}Mn_xN$ thin film made by the molecular beam epitaxy method, which exhibits the mixture of Mn^{2+} (majority) and Mn^{3+} (minority).[24] However, γ-Ga_2O_3 with defective spinel structure has both sites with coordination number (CN) 4 and 6, which can be occupied by either Mn^{2+} or Mn^{3+}. This makes the problem more complicated to clarify the origin of ferromagnetism in this material.

In our previous work, a Mn-$L_{2,3}$ near edge x-ray absorption fine structure (NEXAFS) experiment performed for Mn-doped film revealed that Mn ions take the valence of 2+ with CN=4 in spinel structure.[21] However, the x-ray absorption spectrum measured by the total electron yield method can provide information from the surface layer with only about a few tens of nanometers, which is not enough to examine the film with several hundred nanometers thickness as a whole. In the present work, we examine the valency of Mn by electron energy-loss near edge structure (ELNES). NEXAFS and ELNES by TEM are known to show nearly the same spectra when the instrumental line broadening is deconvoluted.[25]

Figure 10 shows a typical Mn-$L_{2,3}$ ELNES obtained from the center of Mn-doped film using a 20 nm probe. The Mn-$L_{2,3}$ NEXAFS of the same sample[21] is shown for comparison. The Mn-$L_{2,3}$ ELNES has been shifted to align with Mn-$L_{2,3}$ NEXAFS. The position of the L_3 peak at about 640 eV in NEXAFS of the present sample is very close to those of the reference spectra from $Zn_{1-x}Mn_xO$ (x=0.05) (Ref. 24) and MnO,[26] implying that Mn^{2+} is dominant. However, a shoulder peak at the left-hand side of the L_3 peak in the spectrum of MnO with a rocksalt structure (CN=6) is absent in the present sample, suggesting Mn^{2+} with CN=4. This feature was well reproduced by a first-principles multielectron calculation for Mn^{2+} with CN=4.[21] As can be found, the Mn-$L_{2,3}$ ELNES exhibits similar spectral shape as that of

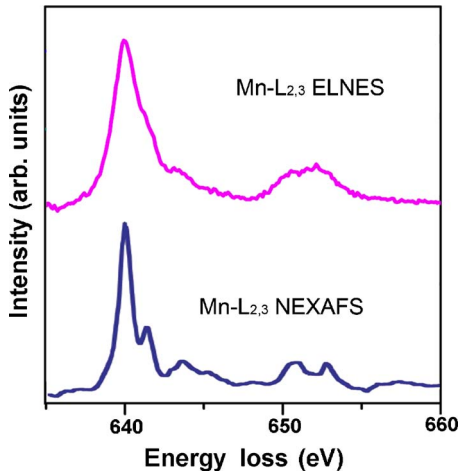

FIG. 10. Typical Mn-$L_{2,3}$ energy-loss near-edge structure from the center of Mn-doped γ-Ga_2O_3 film, compared with Mn-$L_{2,3}$ near-edge x-ray absorption fine structure from the same sample (see Ref. 21).

NEXAFS except for the fact that the linewidth of the ELNES is broader (the energy resolution of NEXAFS and ELNES are about 0.2 and 1.0 eV under the present experimental conditions, respectively). The reliable consistency between ELNES and NEXAFS unambiguously confirms that Mn ions in Mn-doped film take the valence of 2+ with CN=4 in a spinel structure through the whole film.[21]

IV. CONCLUSIONS

Undoped and Mn-doped Ga_2O_3 thin films have been grown on sapphire (0001) plane by pulsed-laser deposition technique. Careful electron diffraction analyses of undoped and Mn-doped thin films found that β-Ga_2O_3 forms in the undoped film with an orientation relationship of $(\bar{2}01)_{\beta\text{-}Ga_2O_3}//(0001)_{Al_2O_3}$, and $[102]_{\beta\text{-}Ga_2O_3}//[2\bar{1}\bar{1}0]_{Al_2O_3}$ or $[\bar{1}0\bar{2}]_{\beta\text{-}Ga_2O_3}//[2\bar{1}\bar{1}0]_{Al_2O_3}$. On the other hand, the Mn-doped film shows γ-Ga_2O_3 phase with defective spinel structure with an orientation relationship of $(\bar{1}11)_{\gamma\text{-}Ga_2O_3}//(000\bar{1})_{Al_2O_3}$, and $[2\bar{1}\bar{1}]_{\gamma\text{-}Ga_2O_3}//[2\bar{1}\bar{1}0]_{Al_2O_3}$ or $[\bar{2}11]_{\gamma\text{-}Ga_2O_3}//[2\bar{1}\bar{1}0]_{Al_2O_3}$. The Mn-doped film shows ferromagnetism at room temperature. Mn ions are uniformly distributed in the film with a concentration of 7.8 cation % and no detectable precipitates are found. Mn-$L_{2,3}$ ELNES reveals that Mn ions take the valency of 2+ and are located at the substitutional site of Ga with CN=4.

ACKNOWLEDGMENTS

This work was supported by three projects by Japanese Ministry of Education, Culture, Sports, Science and Technology (MEXT). They are the computational materials science unit in Kyoto University, the Grant-in-Aid for Scientific Research (A), and the 21st century COE program.

[1] H. Munekata, H. Ohno, S. von Molnar, A. Segmüller, L. L. Chang, and L. Esaki, Phys. Rev. Lett. **63**, 1849 (1989).
[2] H. Ohno, A. Shen, F. Matsukura, A. Oiwa, A. Endo, S. Katsumoto, and Y. Iye, Appl. Phys. Lett. **69**, 363 (1996).
[3] H. Ohno, Science **281**, 951 (1998).
[4] B. Beschoten, P. A. Crowell, I. Malajovich, D. D. Awschalom, F. Matsukura, A. Shen, and H. Ohno, Phys. Rev. Lett. **83**, 3073 (1999).
[5] T. Dietl, H. Ohno, F. Matsukura, J. Cibert, and D. Ferrand, Science **287**, 1019 (2000).
[6] Y. Matsumoto *et al.*, Science **291**, 854 (2001).
[7] P. Sharma *et al.*, Nat. Mater. **2**, 673 (2003).
[8] J. Philip *et al.*, Nat. Mater. **5**, 298 (2006).
[9] J. Okabayashi *et al.*, J. Appl. Phys. **95**, 3573 (2004).
[10] A. K. Pradhan *et al.*, Appl. Phys. Lett. **86**, 152511 (2005).
[11] A. Che Mofor *et al.*, Appl. Phys. Lett. **87**, 062501 (2005).
[12] S. Sonoda, S. Shimizu, T. Sasaki, Y. Yamamoto, and H. Hori, J. Cryst. Growth **237–239**, 1358 (2002).
[13] R. Roy, V. G. Hill, and E. F. Osborn, J. Am. Chem. Soc. **74**, 719 (1952).
[14] S. Geller, J. Chem. Phys. **33**, 676 (1960).
[15] M. Zinkevich, F. M. Morales, H. Nitsche, M. Ahrens, M. Ruhle, and F. Aldinger, Z. Metallkd. **95**, 756 (2004).
[16] M. Orita, H. Ohta, M. Hirano, and H. Hosono, Appl. Phys. Lett. **77**, 4166 (2000).
[17] M. Orita, H. Hiramatsu, H. Ohta, M. Hirano, and H. Hosono, Thin Solid Films **411**, 134 (2002).
[18] K. Matsuzaki, H. Hiramatsu, K. Nomura, H. Yanagi, T. Kamiya, M. Hirano, and H. Hosono, Thin Solid Films **496**, 37 (2006).
[19] H. W. Kim and N. H. Kim, Mater. Sci. Eng., B **110**, 34 (2004).
[20] T. Minami, Solid-State Electron. **47**, 2237 (2003).
[21] H. Hayashi, R. Huang, H. Ikeno, F. Oba, S. Yoshioka, I. Tanaka, and S. Sonoda, Appl. Phys. Lett. **89**, 181903 (2006).
[22] M. F. Chi, H. Gu, X. Wang, and P. L. Wang, J. Am. Ceram. Soc. **86**, 1953 (2003).
[23] D. B. Williams and C. B. Carter, *Transmission Electron Microcopy, IV* (Plenum, New York, 1996), p. 600.
[24] S. Sonoda *et al.*, J. Phys.: Condens. Matter **18**, 4615 (2006).
[25] I. Tanaka, T. Mizoguchi, and T. Yamamoto, J. Am. Ceram. Soc. **88**, 2013 (2005).
[26] B. Gilbert *et al.*, J. Phys. Chem. A **107**, 2839 (2003).